

Mechanical properties of textured, multilayered alumina produced using electrophoretic deposition in a strong magnetic field

Tohru S. Suzuki*, Tetsuo Uchikoshi, Hideo Okuyama, Yoshio Sakka, Keiji Hiraga

Fine Particle Processing Group, Materials Engineering Laboratory, National Institute for Materials Science, 1-2-1 Sengen, Tsukuba, Ibaraki 305-0047, Japan

Available online 18 August 2005

Abstract

The mechanical properties of ceramics materials can be tailored by designing their microstructures. It had generally been difficult to utilize a magnetic field for controlling the texture of diamagnetic ceramics because of their extremely small susceptibility; however, the possibility of controlling the texture by a magnetic field occurred with the development of superconducting magnets. We demonstrate in this study that alumina/alumina laminar composites with alternate crystalline-oriented layers are produced by electrophoretic deposition in a strong magnetic field and that the bending strength of the laminar composite depended on the direction of the multilayered microstructure.

© 2005 Elsevier Ltd. All rights reserved.

Keywords: Suspension; Strength; Al₂O₃; Orientation

1. Introduction

Alumina ceramics have been widely used as structural ceramics, because of their excellent properties such as chemical stability, electrical properties and mechanical properties. Many engineering ceramics are now designed and fabricated with microstructures that exhibit a high strength and toughness.^{1–3} Textured structured ceramics have attracted increasing attention, because of their improved mechanical, electrical and other properties.^{4–6} Many trials have resulted in the production of textured ceramics, including templated grain growth^{4,5,7} and hot forging.^{8–10} We have reported that the development of a textured microstructure in ceramics, such as α -Al₂O₃, TiO₂, ZnO, could be controlled by slip casting in a high magnetic field followed by heating even for diamagnetic ceramics.^{11–14}

A crystal with an anisotropic magnetic susceptibility will rotate to an angle minimizing the system energy when placed in a magnetic field. If the crystal susceptibility parallel to the c axis is $\chi_{//}$, then χ_{\perp} is perpendicular and the difference is $\Delta\chi$.

The magnetic torque, T , attributed to the interaction between the anisotropic susceptibility and magnetic field is estimated from Eq. (1).¹⁵

$$T = \frac{\Delta\chi VB^2}{2\mu_0} \sin 2\theta \quad (1)$$

where V is the volume of each particle, μ_0 the permeability in a vacuum, B the applied magnetic field and θ the angle between an easy magnetization axis in a crystal and imposed magnetic field direction. This is the driving force for magnetic alignment.

The successful control of the development of a textured microstructure in feeble magnetic ceramics was achieved by electrophoretic deposition (EPD) in a strong magnetic field^{16,17} and the combination of the orientation and lamination was one of the possible ways of tailoring the microstructure to improve the mechanical properties and other properties due to the superposition effect.

Hence, we attempted to produce alumina/alumina laminar composites with different crystalline-oriented layers by EPD in a strong magnetic field. The mechanical properties of these laminar composites were then studied.

* Corresponding author. Tel.: +81 29 859 2459; fax: +81 29 859 2401.
E-mail address: suzuki.tohru@nims.go.jp (T.S. Suzuki).

2. Procedure

The starting material was high-purity (>99.99%) spherical, single crystalline α -alumina powder with a particle diameter averaging 0.2 μm . The alumina powder was dispersed in distilled water at pH 4 using an ultrasonic homogenizer and a magnetic stirrer, and then a deflocculated aqueous suspension with a 10 vol% solid content was prepared. The suspension was placed in a superconducting magnet with a room temperature bore of 100 mm, and then a strong magnetic field of 10 T was applied to the suspension to rotate each particle by the magnetic torque attributed to the anisotropic susceptibility as previously described.¹⁶ The magnetic field was maintained in the suspension during the EPD at a constant voltage of 30 V at room temperature. A palladium sheet was used as the cathodic substrate to absorb hydrogen produced by electrolysis of the solvent.¹⁸ A schematic illustration of the apparatus is shown in Fig. 1. The direction of the electric field relative to the magnetic field (the angle between the vectors E and B , φ_{B-E}) was altered ($\pm 45^\circ$) at 3-min intervals to control the dominant crystal faces. After EPD in the strong magnetic field for 50 min, the thickness of the green compacts was approximately 6 mm. These compacts were further densified by cold isostatic pressing (CIP) at 392 MPa and without CIP for reference. The green bodies were then isothermally fired at 1873 K for 2 h in air without the magnetic field.

The bend strength was determined using the 3-point bending test with a span length of 18 mm and a crosshead speed of 0.5 mm/min for samples in which the tensile surface was either parallel or perpendicular to the plane defined by the substrate. Schematic illustrations of the orientation of the

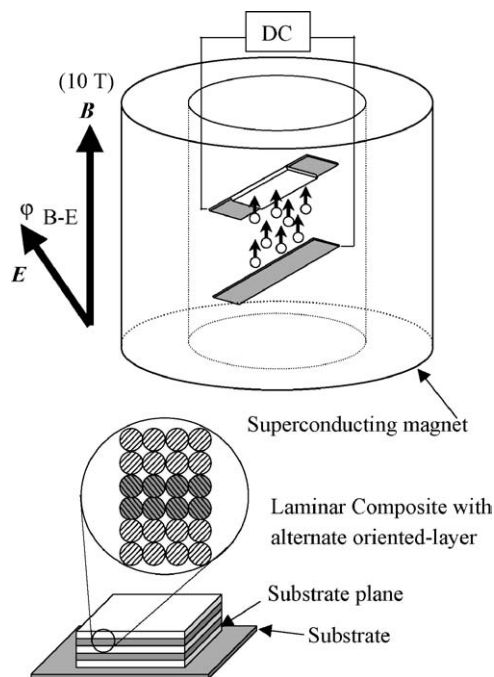


Fig. 1. Schematic illustration of the EPD apparatus in a superconducting magnet.

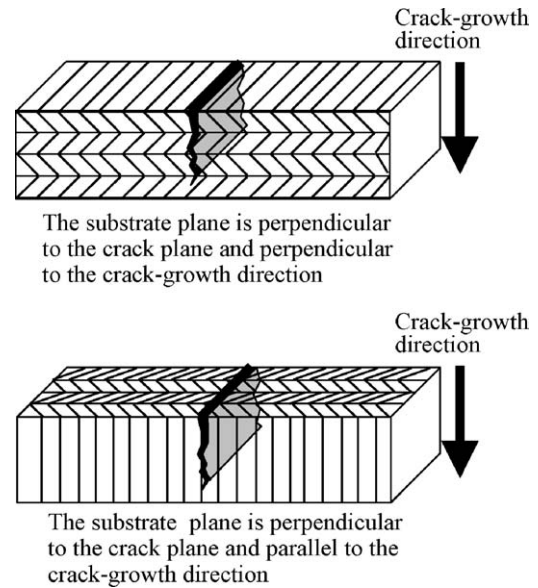


Fig. 2. Schematic illustration of crack growth and bend-bar geometries for alumina specimens with alternate oriented layer.

crack plane relative to the samples are shown in Fig. 2. Two types of samples were tested: (a) laminate alumina composite with the substrate plane perpendicular to the crack plane and perpendicular to the crack-growth direction, and (b) laminate alumina composite with the substrate plane perpendicular to the crack plane and parallel to the crack-growth direction. The fracture toughness was evaluated using the SEPB (single edge precracked beam) method. The precracks were introduced into the SEPB samples using the bridge-indentation method.¹⁹

3. Results and discussion

The green density of the deposits was $\sim 60\%$ of the theoretical density (TD) regardless of the deposition in or out of the magnetic field. The sintered density of the deposits at 1873 K for 2 h was $\sim 97\%$ of the TD without CIP treatment. After CIP treatment was carried out, the density of the specimens sintered at 1873 K for 2 h was $\sim 98\%$ of the TD regardless of the deposition in or out of the magnetic field. Fig. 3 shows a macroscopic view of the sample surface after being consolidated by EPD. A bubble-free and flat surface was observed. The use of a palladium substrate effectively suppressed the bubble formation at the cathode and dense, bubble-free deposits were obtained.

Fig. 4(a) and (b) show the cross-sectional microstructures of alumina prepared by the EPD with and without applying a magnetic field. The microstructure of a specimen not subjected to a magnetic field are shown in Fig. 4(a). It can be seen that the grains appear randomly distributed in the untextured alumina. A schematic illustration and the microstructure of the alumina/alumina laminate composite with alternate crystalline-oriented layers are shown in

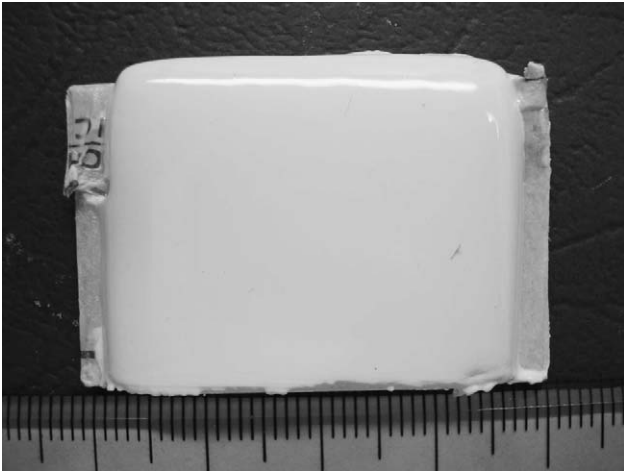


Fig. 3. Macroscopic view of the sample surface after consolidated by EPD.

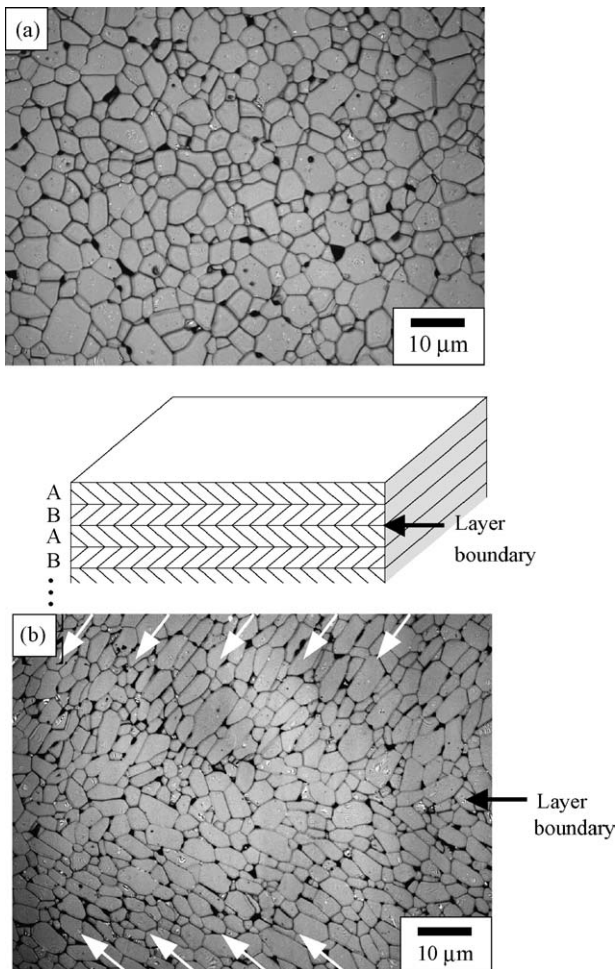


Fig. 4. Microstructure of the cross-section: (a) alumina prepared by EPD without a magnetic field, (b) an alumina/alumina laminate composite prepared by alternately changing $\varphi_{B-E} = \pm 45^\circ$ during EPD in a magnetic field of 10 T.

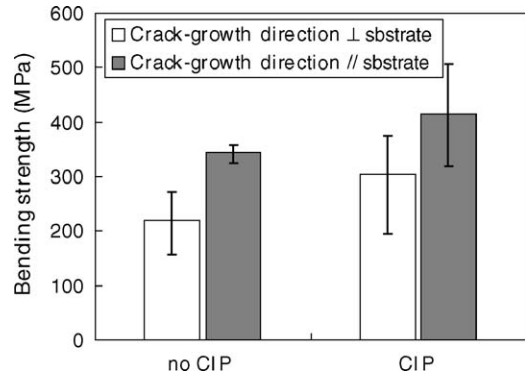


Fig. 5. Bending strength for laminate alumina composite with alternate oriented layer, depending on the crack-growth direction.

Fig. 4(b). This composite was fabricated by alternately changing the angle between the directions of the magnetic and electric fields ($\varphi_{B-E} = \pm 45^\circ$) layer by layer during the EPD in 10 T. The grains in the alternate layers are aligned differently as indicated by the arrows in Fig. 4. We have already confirmed^{11,16} that the *c* axis of alumina with the trigonal unit cell was parallel to the direction of the magnetic

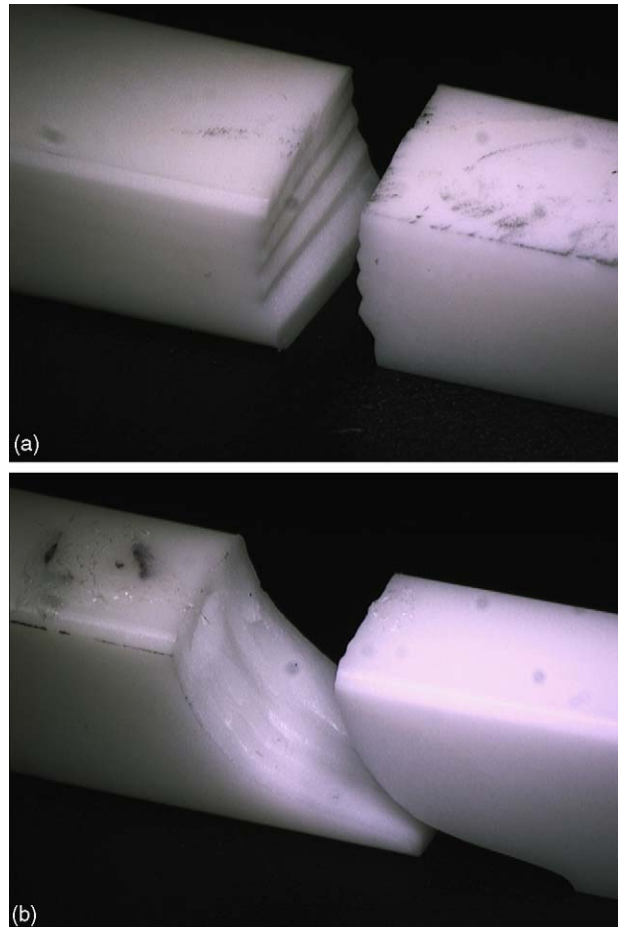


Fig. 6. Macroscopic views of the alumina/alumina laminate composites after the bending test: (a) crack-growth direction perpendicular to the substrate plane, and (b) crack-growth direction parallel to the substrate plane.

field. Consequently, the direction of the c axis in the alternate layer can be controlled by the EPD in a strong magnetic field.

The bending strengths for specimens with CIP and without CIP are shown in Fig. 5. CIP treatment increases the bending strength because the residual defects in the specimens were reduced after sintering. The bending strength depends on the crack-growth direction. The strength for the crack-growth direction parallel to the substrate was higher than that perpendicular to the substrate even with or without CIP treatment.

Fig. 6(a) and (b) are macroscopic views of the specimens after the bending test. In Fig. 6(a), the crack-growth direction was perpendicular to the substrate, while in Fig. 6(b), the crack-growth direction was parallel to the substrate. A crack was propagated by bending in a zigzag path along the aligned grain in the alternate crystalline-oriented layers when the crack-growth direction was perpendicular to the substrate (Fig. 6(a)). In Fig. 6(b), the crack changed to the direction perpendicular to the initial crack-growth.

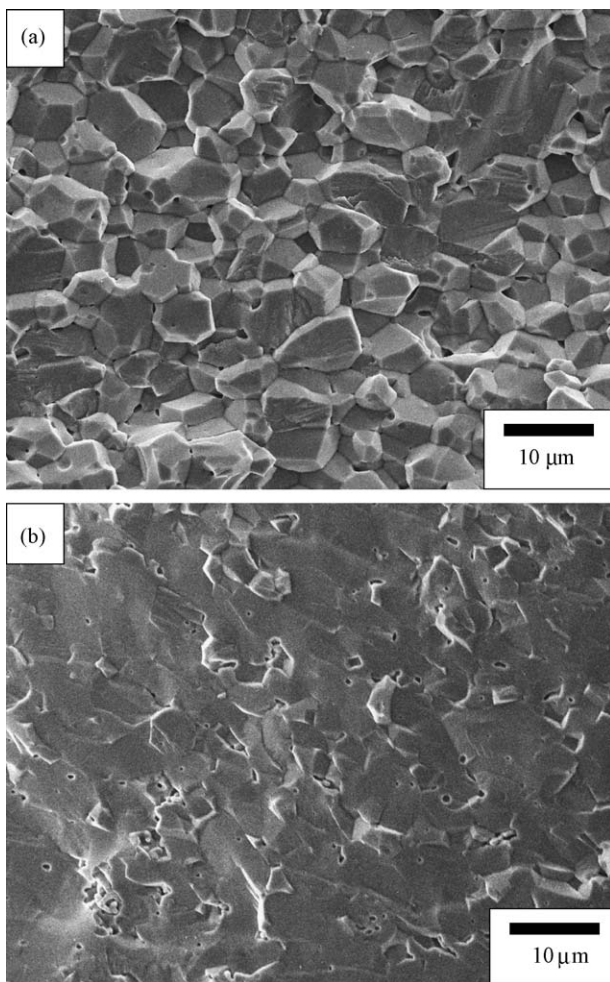


Fig. 7. SEM observation of fractured surfaces of the alumina/alumina laminate composites after the bending test: (a) crack-growth direction perpendicular to the substrate plane and (b) crack-growth direction parallel to the substrate plane.

The scanning electron micrographs shown in Fig. 7 reveal two distinct crack morphologies on the fracture surfaces for the alumina laminate composite with alternate oriented layers, which depended on the crack-growth direction. A complete intergranular mode of fracture was observed when the loading direction was perpendicular to the substrate (Fig. 7(a)). It is very difficult to propagate a crack along the basal plane in alumina at room temperature,²⁰ thus the crack propagated along the grain boundary parallel to the basal plane. In contrast, the fracture surface was dominated by the intragranular mode when the crack-growth direction was parallel to the substrate as shown in Fig. 7(b).

Fracture toughness values (K_{IC}) were 4.99 and 3.65 MPa m^{1/2} for the crack-growth directions parallel and perpendicular to the substrate, respectively. The fracture toughness for the crack-growth direction parallel to the substrate was higher than that perpendicular to the substrate. The fracture toughness depended on the crack-growth direction, in the same manner as the bending strength.

4. Summary

We attempted to produce alumina/alumina laminar composites with different crystalline-oriented layers by EPD in a strong magnetic field, and then evaluated their mechanical properties.

The crystalline orientation in alternative layers can be controlled by EPD and a strong magnetic field. Both the bending strength and fracture toughness for the crack-growth direction parallel to the substrate were higher than those for the crack-growth direction perpendicular to the substrate. The fracture mode depended on the crack-growth direction.

Acknowledgements

This work was partially supported by the Budget for Nuclear Research of the Ministry of Education, Culture, Sports, Science and Technology (MEXT) and a MEXT, Grant-in-Aid for Scientific Research.

References

1. Rani, D. A., Yoshizawa, Y., Hirao, K. and Yamauchi, Y., Effect of rare-earth dopants on mechanical properties of alumina. *J. Am. Ceram. Soc.*, 2004, **87**, 289–292.
2. Hirao, K., Ohashi, M., Brito, M. E. and Kanzaki, S., Processing strategy for producing highly anisotropic silicon nitride. *J. Am. Ceram. Soc.*, 1995, **78**, 1687–1690.
3. Waku, Y., Nakagawa, N., Wakamoto, T., Ohtsubo, H., Shimizu, K. and Kohtoku, Y., A ductile ceramics eutectic composite with high strength at 1,873 K. *Nature*, 1997, **389**, 49.
4. Carisey, T., Levin, I. and Brandon, D. G., Microstructure and mechanical properties of textured Al₂O₃. *J. Eur. Ceram. Soc.*, 1995, **15**, 283–289.

5. Takeuchi, T., Tani, T. and Saito, Y., Piezoelectric properties of bismuth layer-structured ferroelectric ceramics with a preferred orientation processed by the reactive templated grain growth method. *Jpn. J. Appl. Phys.*, 1999, **38**, 5553–5556.
6. Hirao, K., Watari, K., Brito, M. E., Toriyama, M. and Kanzaki, S., High thermal conductivity in silicon nitride with anisotropic microstructure. *J. Am. Ceram. Soc.*, 1996, **79**, 2485–2488.
7. Seabaugh, M. M., Kerscht, I. H. and Messing, G. L., Texture development by templated grain growth in liquid-phase-sintered α -alumina. *J. Am. Ceram. Soc.*, 1997, **80**, 1181–1188.
8. Yoshizawa, Y., Toriyama, M. and Kanzaki, S., Fabrication of textured alumina by high-temperature deformation. *J. Am. Ceram. Soc.*, 2001, **84**, 1392–1394.
9. Ma, Y. and Bowman, K. J., Texture in hot-pressed or forged alumina. *J. Am. Ceram. Soc.*, 1991, **74**, 2941–2944.
10. Takenaka, T. and Sakata, K., Grain orientation and electrical properties of hot-forged $\text{Bi}_4\text{Ti}_3\text{O}_{12}$ ceramics. *Jpn. J. Appl. Phys.*, 1980, **19**, 31–39.
11. Suzuki, T. S., Sakka, Y. and Kitazawa, K., Orientation amplification of alumina by colloidal filtration in a strong magnetic field and sintering. *Adv. Eng. Mater.*, 2001, **3**, 490–492.
12. Suzuki, T. S. and Sakka, Y., Fabrication of textured titania by slip casting in a high magnetic field followed by heating. *Jpn. J. Appl. Phys.*, 2002, **41**, L1272–L1274.
13. Suzuki, T. S. and Sakka, Y., Control of texture in ZnO by slip casting in a strong magnetic field and heating. *Chem. Lett.*, 2002, 1204–1205.
14. Sakka, Y., Suzuki, T. S., Tanabe, N., Asai, S. and Kitazawa, K., Alignment of titania whisker by colloidal filtration in a high magnetic field. *Jpn. J. Appl. Phys.*, 2002, **41**, L1416–L1418.
15. Sugiyama, T., Tahashi, M., Sassa, K. and Asai, S., The control of crystal orientation in non-magnetic metals by imposition of a high magnetic field. *ISIJ Int.*, 2003, **43**, 855–861.
16. Uchikoshi, T., Suzuki, T. S., Okuyama, H. and Sakka, Y., Control of crystalline texture in polycrystalline alumina ceramics by electrophoretic deposition in a strong magnetic field. *J. Mater. Res.*, 2004, **19**, 1487–1491.
17. Uchikoshi, T., Suzuki, T. S., Okuyama, H. and Sakka, Y., Electrophoretic deposition of α -alumina particles in a strong magnetic field. *J. Mater. Res.*, 2003, **18**, 254–256.
18. Uchikoshi, T., Ozawa, K., Hatton, B. D. and Sakka, Y., Dense bubble-free ceramics deposits from aqueous suspension by electrophoretic deposition. *J. Mater. Res.*, 2001, **16**, 321–324.
19. Nose, T. and Fujii, T., Evaluation of fracture toughness for ceramics materials by a single-edge-precracked-beam method. *J. Am. Ceram. Soc.*, 1988, **71**, 328–333.
20. Becher, P. F., Fracture-strength anisotropy of sapphire. *J. Am. Ceram. Soc.*, 1976, **59**, 59–61.